PNAS
www.pnas.org

Supplementary Information for

Transferrin receptor binds capsids with dynamic motion: receptor and virus rock and roll

Hyunwook Lee, Heather M. Callaway, Javier O. Cifuente, Carol M. Bator, Colin R. Parrish, Susan L. Hafenstein

Susan L. Hafenstein
Email: suh21@psu.edu

This PDF file includes:

Supplementary text
Figures S1 to S10
Tables S1
Legends for Movies S1 to S5
SI References

Other supplementary materials for this manuscript include the following:

Movies S1 to S5

www.pnas.org/cgi/doi/10.1073/pnas.1904918116

SI Materials and Methods

Normal mode analysis. NMA in internal coordinates (IC) was performed by using iMOD (1). First, 'imode' was run on the fitted atomic model of CPV-TfR-Tf complex with coarse-grained model and 72% of dihedrals were randomly removed. The resulting PDB model for the peptide backbone and IC normal modes file were used as input for "imove" to animate the modes (mode 1, 2, and 3). The animated normal modes were visualized by using VMD (2).

Bio-layer interferometry binding experiments with Tf bound and unbound TfR. In order to remove Tf from the bbj-TfR, purified TfR was incubated with 50mM deferiprone (3-Hydroxy-1,2-dimethyl-4(1H)-pyridone) in PBS (pH 7.4) for 5 min and then buffer exchanged into 0.1M pH 5.5 citric acid using a 30kDa Amicon concentrator in order to cause TfR and Tf to disassociate. Samples were then buffer exchanged into PBS with a Amicon Ultracel-30 membrane filter (Millipore) and incubated with Ni-NTA beads, which were then washed in PBS to remove Tf. Ni-NTA beads were eluted with 250mM imidazole to release TfR, and TfR was buffer exchanged into PBS with a 30kDa Amicon concentrator for binding studies.

Bio-layer interferometry binding experiments were performed in a BLItz bio-layer interferometer (Fortebio). Ni-NTA biosensors (Fortebio) were hydrated in kinetics buffer (PBS, pH 7.4 with 0.02% ovalbumin and 0.02% Tween-20) for 10 minutes at room temperature, and then loaded onto the bio-layer interferometer. Experiments were performed as follows: biosensors were incubated in kinetics buffer for 30s (baseline measurement), incubated with either 2.5μg/mL Tf-free TfR or 5μg/mL Tf:TfR complex (equal molar concentration of TfR in each sample) for 300s, washed in kinetics buffer for 60s to remove unbound receptor, then incubated with CPV empty capsids (240μg/mL) for 300s (association step), and washed in kinetics buffer for 300s (disassociation step).

Charge detection mass spectrometry. The TfR purified preparation was assessed using charge detection mass spectrometry as described previously (3). Briefly, ions are produced by a nanoelectrospray source (Advion Biosciences) and introduced into the instrument through a heated metal capillary. Ions pass through three differentially pumped regions containing an ion funnel, a hexapole, and a quadrupole. The nominal ion energy of 100 eV/z is set by the static potential applied to the hexapole. The ions are then focused into a dual hemispherical deflection energy analyzer (HDA). The HDA transmits ions within a narrow band of kinetic energies centered on 100 eV/z. The transmitted ions are focused into an electrostatic linear ion trap with a cylindrical charge detector tube at its center. The trap end-cap voltages are raised, and a trapping event occurs. After a user determined time (100 ms for these experiments), the end-caps are grounded and the trap is emptied. During a trapping event the ion oscillates back and forth through detector tube, inducing a periodic signal which is amplified, digitized and transferred to a computer for analysis. The digitized signals were analyzed by a Fortran program using fast Fourier transforms. Events where ions were not trapped for the whole trapping time were discarded.

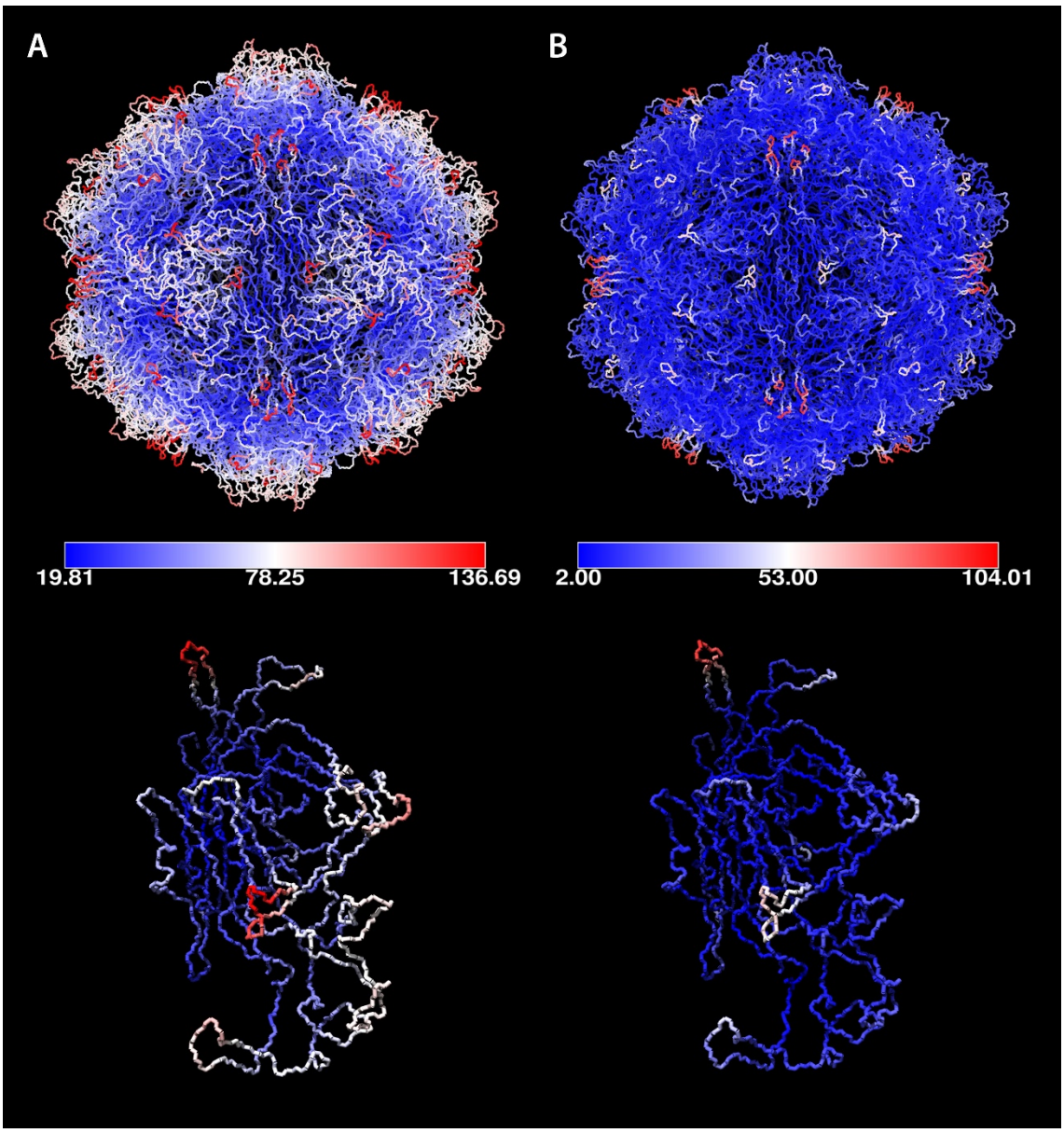

Fig. S1. The B-factor differences between receptor bound versus non-bound capsids. The atomic models for the (A) receptor bound capsid and (B) non-bound capsid (PDB ID 2CAS) were represented in wireframe and colored from blue to red according to the keys. VP2s from each capsid were visualized at the bottom.

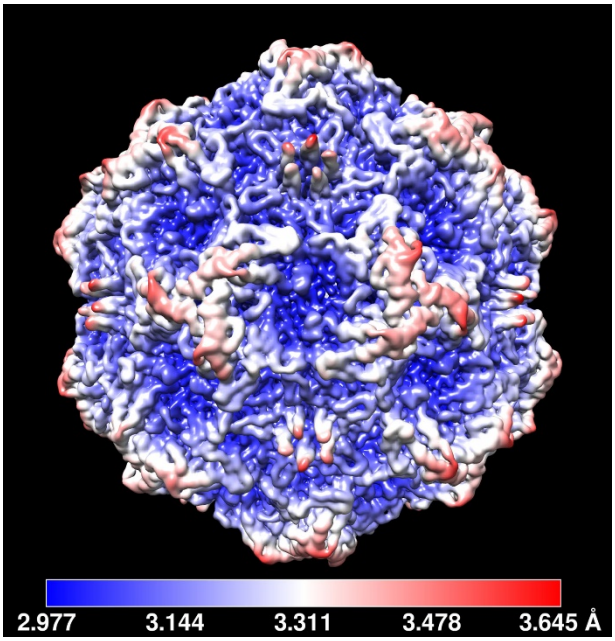

Fig. S2. Local resolutions of the icosahedral map of the capsids in the CPV-TfR complex, determined by full icosahedral averaging. The surface was colored according to key.

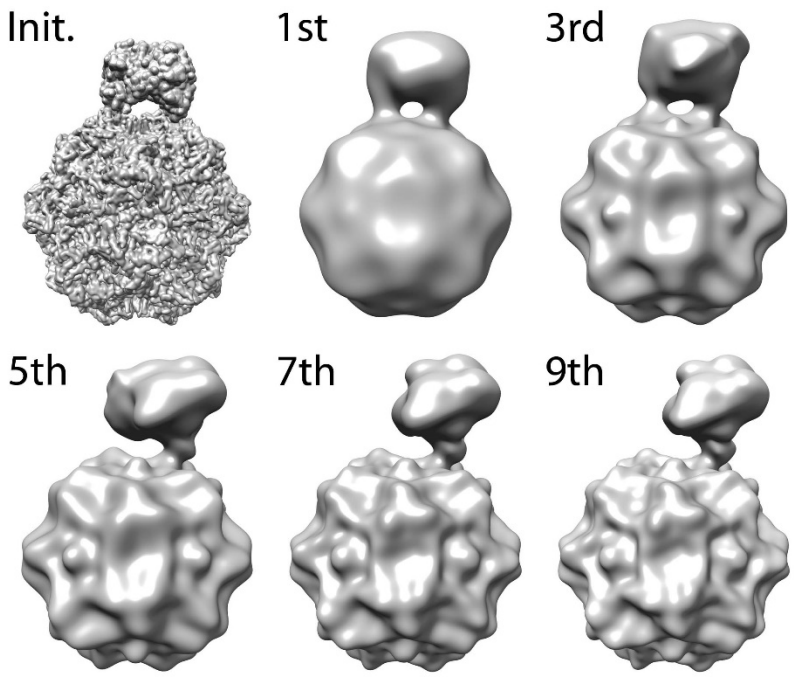

Fig. S3. The progress of the symmetry-mismatch reconstruction. Surface renderings of the representative maps during symmetry-mismatch reconstruction iterations. The initial map was low-pass filtered at 60 Å prior to use.

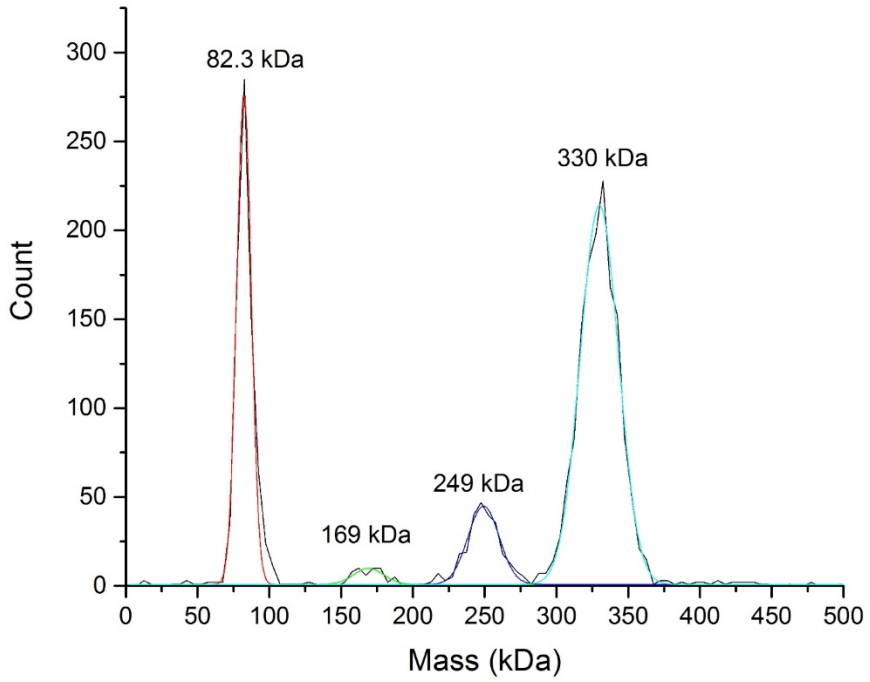

Fig. S4. CDMS (charge detection mass spectrometry) analysis of purified TfR shows free TfR (169 kDa), TfR with one Tf molecule bound (249 kDa) and TfR with two Tf molecules bound (330 kDa). The peak at the left most (82.3 kDa) is likely monomeric TfR and Tf produced during the CDMS experiment.

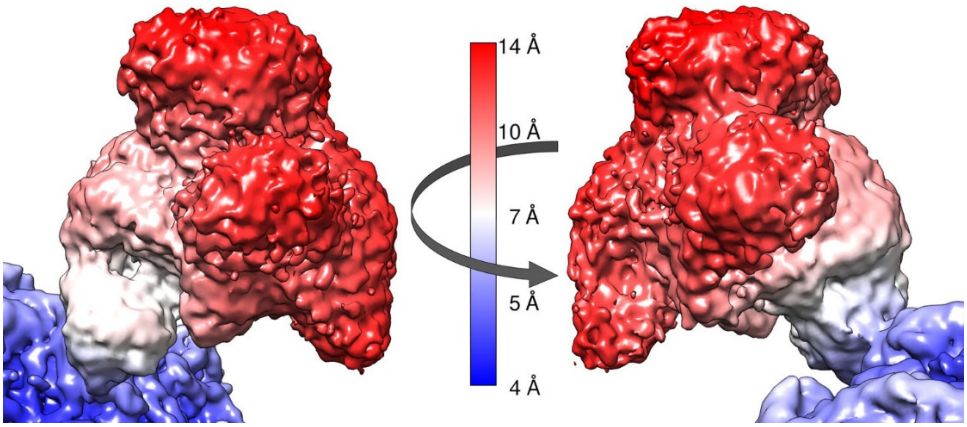

Fig. S5. Local resolutions of the asymmetric map of CPV-TfR complex, produced by symmetry-mismatch reconstruction. The left image is in the same orientation as Figure 2B (lower) and the right image is 180° rotated. The surface was colored according to the color key.

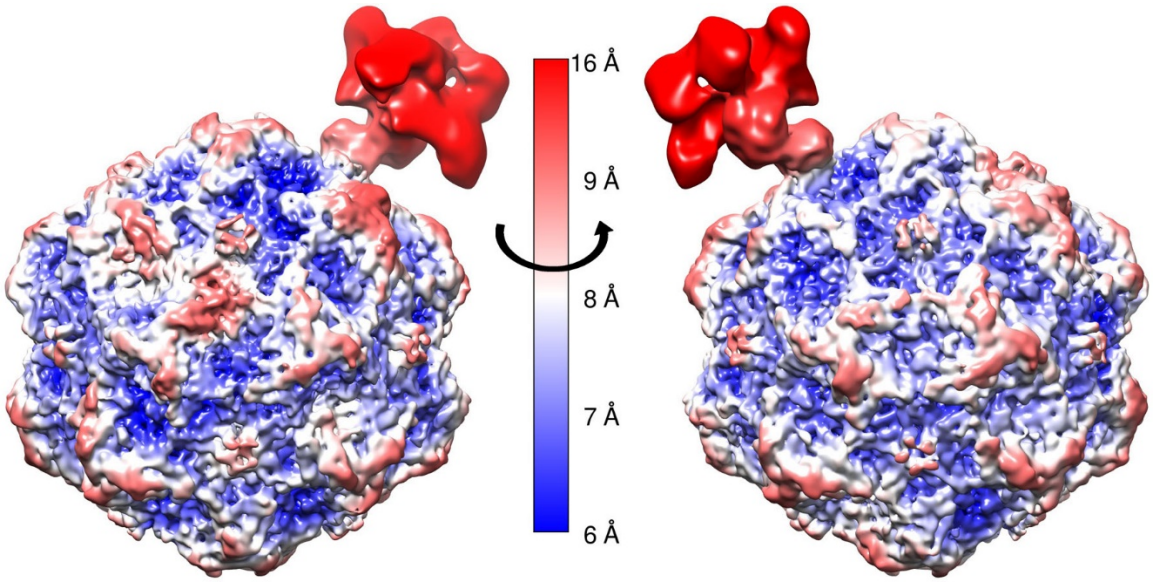

Fig. S6. Local resolutions of the asymmetric map of CPV-TfR complex, generated by using the particles interacting with only one receptor. The left and right panels show opposite sides of the complex. The map was filtered according to the local resolutions by using RELION. The surface was colored according to the color key.

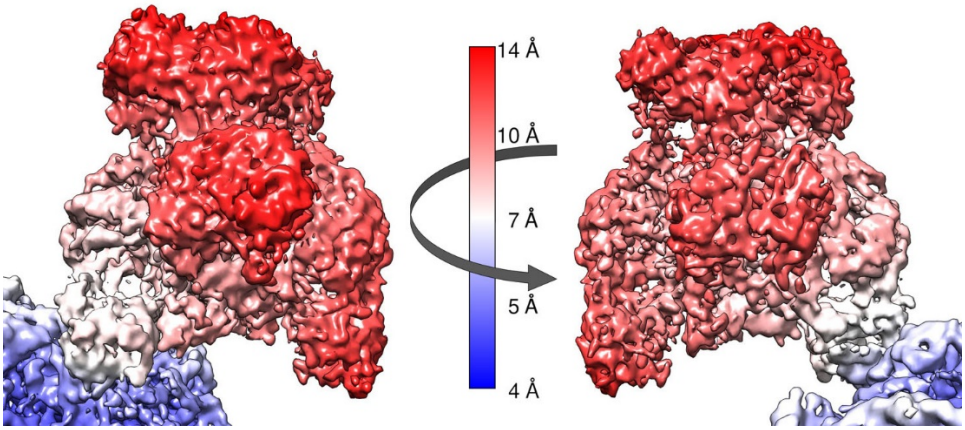

Fig. S7. Local resolutions of the asymmetric map of CPV-TfR complex, generated by using the particles of the class #3 in Fig. 5A. The images are in the same orientations as in Fig. S5. The surface was colored according to the color key.

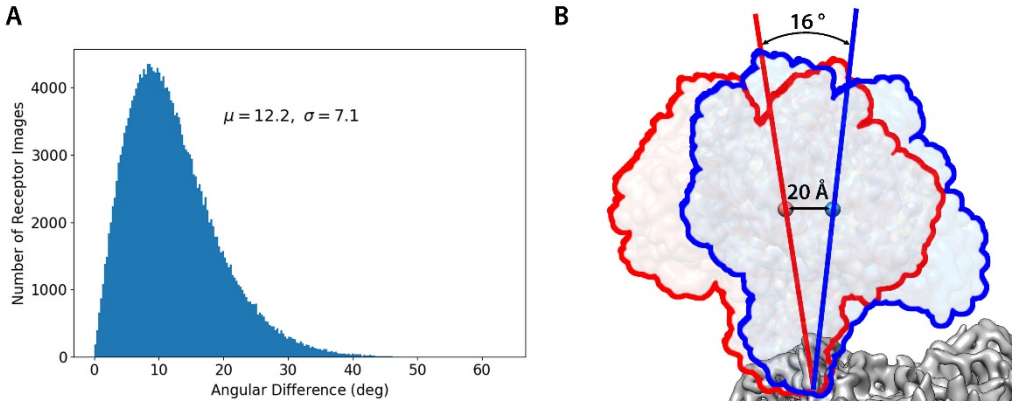

Fig. S8. Swaying motion of the bound receptors in degrees. (A) The angular differences of each receptor before and after the 3D refinement were calculated from the corresponding particle orientations. (B) The angle and distance formed between the two furthest classes.

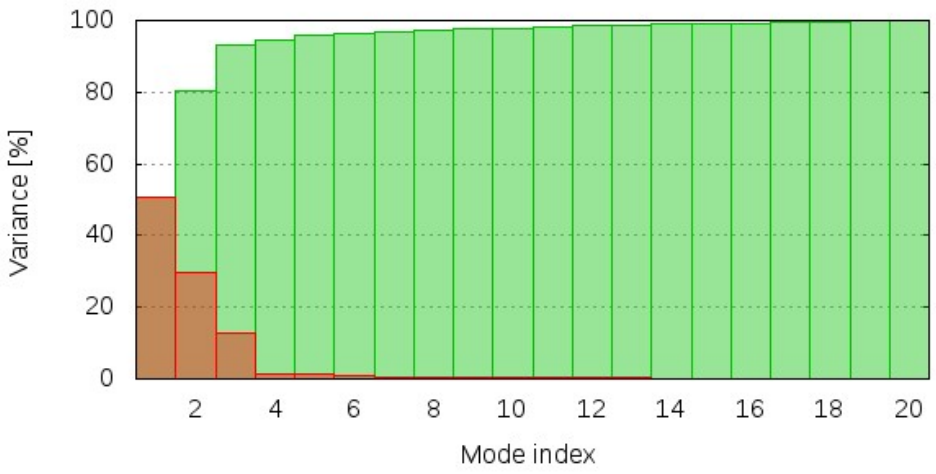

Fig. S9. Variance of NMA modes. The variance associated with each normal mode is inversely related to the eigenvalue. Colored bars show the individual (red) and cumulative (green) variances.

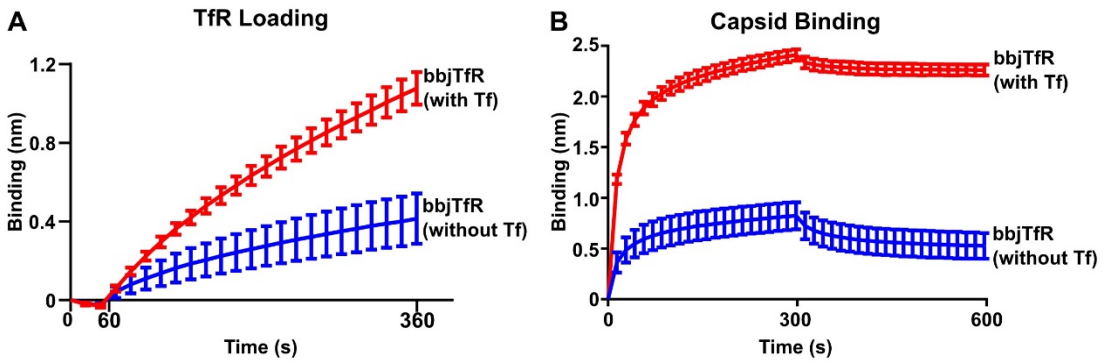

Fig. S10. Bio-layer interferometry was used to examine the relative binding and release of CPV capsids to bbjTfR with or without bound Tf. Based on the molecular masses of the free TfR versus the TfR:Tf complex, equal molar amounts of bbjTfR with (red) or without bound Tf (blue) were incubated with Ni-NTA conjugated bio-layer interferometry probes. Panel A indicates TfR binding to the probe, showing that there was approximately the same number of binding sites present (A, t=60-360s) **(5)**. Probes were washed in kinetics buffer, and then incubated with CPV capsids (240 µg/mL) (t=0-300s; association step) and washed in kinetics buffer (t=301-600s; disassociation step) (B).

Table S1. Cryo-EM data collection, refinement and validation statistics

	CPV + TfR (EMDB-20001)	CPV + TfR (EMDB-20002)	CPV + TfR (EMDB-20002)	TfR (EMDB-20003)
Data collection and processing				
Magnification	x59,000			
Voltage (kV)	300			
Electron exposure (e–/Å^2)	166			
Defocus range (μm)	0.5 – 4.5			
Pixel size (Å)	1.11			
Symmetry imposed	Icos	SMR*	SEF*	LR*
Initial particle images (no.)	158,681	132,120	3,720,300 (62,005)	227,608
Final particle images (no.)	132,120	62,005	227,608	227,608
Map resolution (Å)	3.0	6.2 (8.8)	4.6 (6.4)	6.7
FSC threshold	0.143	0.143 (0.5)	0.143 (0.5)	0.143

	CPV (PDB 6OAS)	TfR
Refinement		
Model composition	capsid (asu)	
Non-hydrogen atoms	261,180 (4,353)	10,172
Protein residues	32,880 (548)	1,280
Ligands	CA	
B factors (Å^2)		
Protein	52.43	373.87
R.m.s. deviations		
Bond lengths (Å)	0.006	0.009
Bond angles (°)	0.739	1.319
Validation		
MolProbity score	1.70	2.66
Clashscore	2.60	23.27
Rotamer outliers (%)	5.67	1.90
Ramachandran plot		
Favored (%)	97.62	88.64
Outliers (%)	0.00	0.24

The marked reconstructions are the results from the image processing methods below:
*SMR: symmetry-mismatch reconstruction
*SEF: symmetry-expanded focused reconstruction
*LR: localized reconstruction
(asu): asymmetric unit

Movie S1 (separate file). Morph analysis generated from the fitted receptor structures into the five 3D classes. The capsid (green), TfR (yellow), Tf (orange) are shown in ribbon diagram.

Movie S2 (separate file). Morph analysis generated from the fitted receptor structures into the five 3D classes. 90° rotated from Movie S1.

Movie S3 (separate file). Surface rendered result of the NMA analysis. Normal mode 1.

Movie S4 (separate file). Surface rendered result of the NMA analysis. Normal mode 2.

Movie S5 (separate file). Surface rendered result of the NMA analysis. Normal mode 3.

References

1. Lopéz-Blanco JR, Garzón JI, Chacón P (2011) iMod: multipurpose normal mode analysis in internal coordinates. *Bioinformatics* 27(20):2843–2850.

2. Humphrey W, Dalke A, Schulten K (1996) VMD: Visual molecular dynamics. *Journal of Molecular Graphics* 14(1):33–38.

3. Dunbar CA, Callaway HM, Parrish CR, Jarrold MF (2018) Probing Antibody Binding to Canine Parvovirus with Charge Detection Mass Spectrometry. *J Am Chem Soc* 140(46):15701–15711.

4. Callaway HM, et al. (2018) Complex and dynamic interactions between parvovirus capsids, transferrin receptors and antibodies control cell infection and host range. *Journal of Virology*:JVI.00460-18.

5. Concepcion J, et al. (2009) Label-Free Detection of Biomolecular Interactions Using BioLayer Interferometry for Kinetic Characterization. *CCHTS* 12(8):791–800.